Thermal performance of the Atlas SCT forward modules

A. Clark [a], M. Donegà [a 1], I. Nasteva [b], S. Snow [b 2], R. Wallny [c], I. Wilmut [d]

[a] *Univérsite de Genève*

[b] *University of Manchester*

[c] *CERN (European Council for Nuclear Research)*

[d] *RAL (Rutherford Appleton Laboratories)*

Abstract

We describe the thermal design of the Atlas SCT forward modules and their cooling blocks. We report on the performance of the C_3F_8 evaporative cooling system and the blocks alone, then on the performance of an irradiated inner module mounted on two alternative prototype cooling blocks (baseline and PEEK split). Runs are presented at different cooling conditions, representative of those expected to be used in the final experiment. We have also measured thermal runaway, with the module mounted on the PEEK split block and cooled with liquid cooling.

[1] *Email address:* mauro.donega@cern.ch

[2] *Email address:* steve@hep.man.ac.uk

28 May 2003

Contents

1 Introduction

All the modules of the SCT (ATLAS Silicon Tracker) have to meet mechanical, thermal and electrical specifications in order for the system to work efficiently and reliably. The thermal specifications are described in reference [1]. They aim at assuring the best possible working conditions for the module when it is dissipating the maximal electrical power. The module will operate in nitrogen atmosphere and it is estimated that it will receive from the environment at most an additional heat load of 0.2 W per detector, coming from radiation and convection. The inner module having only two detectors will collect from the environment 0.4 W, while the outer and middle modules, with four detectors, 0.8 W.
The thermal specifications can be summarized as:

- when the module is dissipating 7 W on the read-out electronics, 185 $\mu W/\mathrm{mm}^2$ at 0°C on the detectors and is subjected to the environment heat load, the detectors have to be cooler than -7°C
- when the power on the hybrid is 7 W and the module is charged with the environmental heat load, thermal runaway must not occur unless the detector power density is above 240 $\mu W/\mathrm{mm}^2$ at 0°C .

The first specification aims at reducing the electronic noise and getting the most favorable annealing condition.
The second specifications set a strict limit on the thermal runaway. The power dissipated by the silicon detectors is related to their temperature, following the equation:

$$I_{leak}(T) \propto T^2 e^{\frac{-E_g}{2K_B T}} \tag{1}$$

where T is the temperature on the detectors, E_g is the *effective* charge carrier activation energy of the silicon after irradiation ($\sim$1.2 eV) and K_B the Boltzmann constant. The power dissipated by the detectors increases their temperature, so the leakage current increases and with it the power dissipation. If the cooling system is able to remove the power dissipated by the detectors, this loop will reach a stable condition, if not, it will diverge. This condition is commonly named *thermal runaway*. Since the thermal runaway represents a dramatic failure of the module that will oblige the user to switch it off, the specification on it is conservative and requires the module to be able to stand 30% more than the maximal power density on the detectors before failing.
The cooling system chosen for the SCT is a two phase evaporative refrigerator cycle based on C_3F_8. The present design of the cooling system is capable of providing temperatures from -14°C down to -30°C on the cooling blocks at zero load. In the SCT there will be three types of forward modules named following their radial position on the disk; inner, middle and outer. Outer and middle modules have four detectors and an approximate length of 16 cm, while the inner one has only two detectors and a length of 10cm. To assure the hermeticity of the SCT, the modules will be mounted with a certain overlap. This condition is implemented by mounting the modules alternately on high and low cooling blocks. Thus, while the layout of the main cooling block is the same for all the modules, half of them will be mounted on "low blocks" 6.6 mm high, while the remaining ones on "high blocks" 12.1 mm high. The thermal resistance of the cooling block is proportional to its thickness; to prove the efficiency of the block design we chose to do all of our tests on the worst case, the high version of the block. Furthermore, outer and middle

modules have a second cooling block at the extremity of the detectors while the inner module, shorter than the others, will only have a second, non-cooled, mounting point. Since the heat dissipated by the inner module detectors will be removed only at the main cooling point, this module is thermally the most critical case, so we choose to test it to prove the efficiency of the cooling design.
A dedicated system has been developed in order to monitor the temperatures of the module and the environment with the module fully operational. Data from runs at different environment conditions have been collected in order to prove different aspects of the cooling design.

2 Thermal design concept

The thermal design of the SCT endcaps has been driven by a few key considerations. Each module can be simplified as two coupled thermal entities:

- Hybrid: maximal power dissipated 7 W. It should operate at the lowest possible temperature to keep down the electronic noise of the ASICs, which rises by about 30 electrons per degree after irradiation. It must always be kept below 40°C , which represents the maximal operating temperature for the ABCD3TA read-out chips [2]. The chosen target for the operating temperature is 2°C .
- Detectors: power is dissipated proportional to radiation damage and operating voltage and power rises exponentially with temperature. The operating power consumption of the detectors is actually limited to 2.5 W (because of the current limit of 5 mA of the HV system at the maximum detector bias of 500V)

The geometry of the modules has been optimized to facilitate the heat extraction and aims at reducing the heat flow from the high temperature hybrid to the low temperature detectors. The operating temperature of the hybrid should be ∼2°C while from specifications the temperature of the detectors has to be below -7°C . The thermal design aims at keeping separate thermal paths from the hybrid and detectors, all the way down to the coolant. Looking at the thermal design, the modules can be divided into two sets. Inner modules having a single cooling block, which is mounted between the hybrid and the detectors and divided into two halves (detector side and hybrid side). Outer and middle modules using the same kind of main cooling block but taking advantage of a second cooling block at the far end (see figure 1). The power dissipated from the detectors is collected by the TPG spine [3] (Thermal Pyrolytic Graphite) going all along the detectors length and injected in the cooling blocks.
For all modules the power dissipated by the hybrid flows to the hybrid half of the main cooling block. The biggest thermal resistance outside the module is at the interface between the block and the cooling fluid (Heat Transfer Coefficient), so the heat paths should be kept separate right up to the fluid if the split block concept is to work well. There have been different split block concepts presented. A common issue about all block designs is the coupling through the underlying pipe and solder layer. The guideline in the choice of the pipe and solder is to reduce their radial thermal resistance (from the coolant to the block) and to increase the thermal resistance between the two halves of the block. Since the solder has a low thermal resistance, to reduce the coupling across the two sides of the block, its thickness is reduced to $\sim 100\ \mu$m. The pipe has two degrees of freedom: thickness and material. The material chosen is CuNi, a low

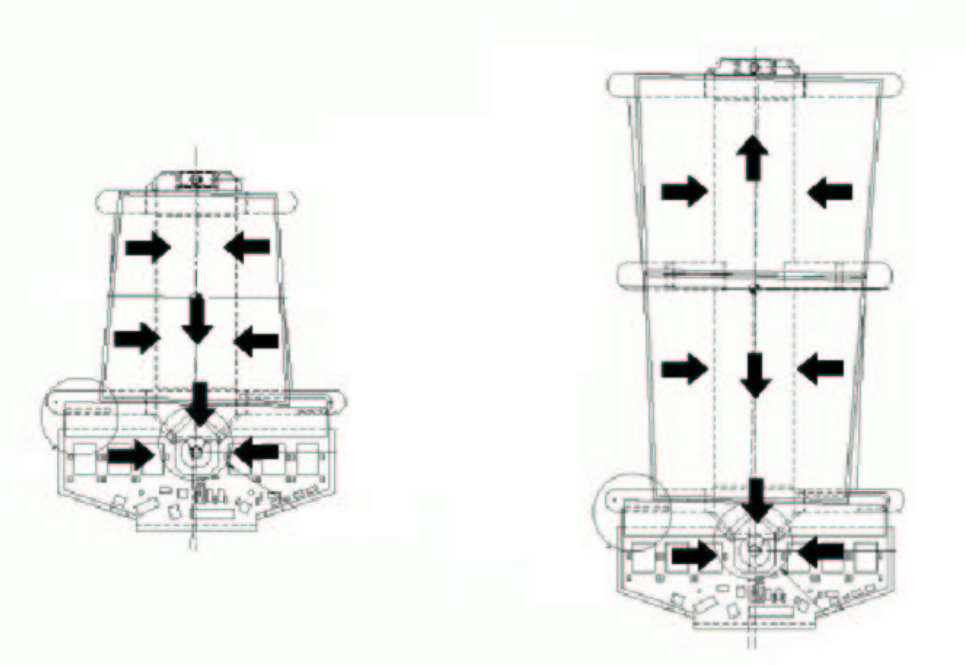

Fig. 1. Innner (left) and outer (right) module thermal design concept.

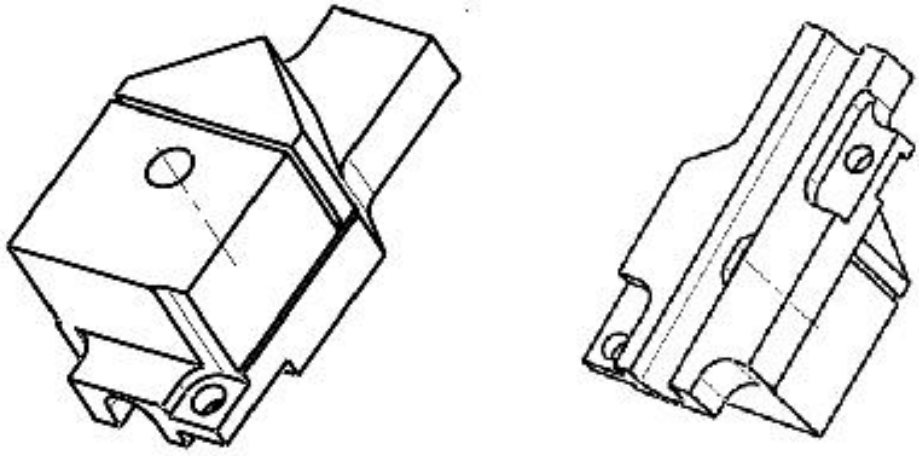

Fig. 2. Main cooling block drawings

thermal conductivity metal alloy (∼29 W/mK) to reduce the coupling between the two halves of the block but, to keep a reasonably low radial thermal resistance, the thickness of the pipe has been reduced to ∼70μm making this object rather fragile.
The choice of the cooling block material aims at reducing both its thermal resistivity and its radiation length. The actual material is a two-dimensional Carbon-Carbon (CC) material having highly conductive fibers in one plane (∼120 W/mK), and lower conductivity in the orthogonal direction (∼70 W/mK).
Three different block concepts have been tested:

- "fully split" block made of two physically separated pieces of CC

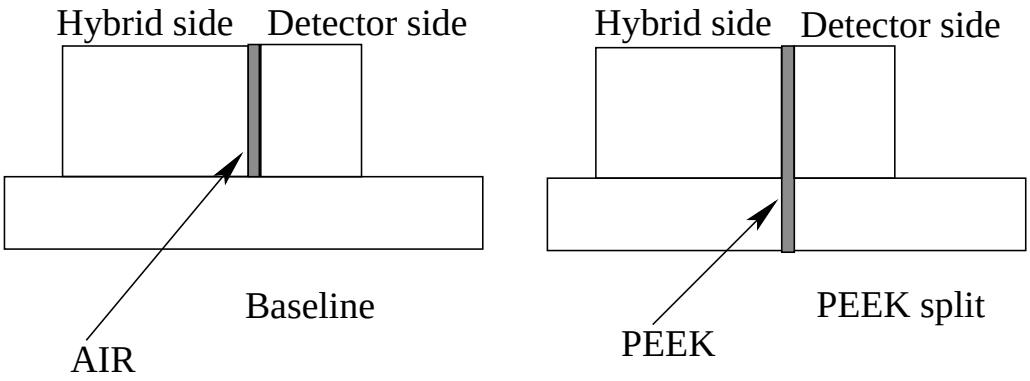

Fig. 3. Thermal path split applied to the main cooling block. Left: baseline block; Right: PEEK split block

- "baseline" block (see figure 2) a single piece of CC with a narrowing of the block between the two halves.
- "PEEK split" block made of a piece of PolyEtherEtherKetone (PEEK) sandwiched between two pieces of CC

The details of the cross sections can be seen in figure 3. The fully split block represents the ideal decoupling between the two halves. The baseline block implements the split concept by creating a bottleneck between the two sides of the block. In the PEEK split block the separation of the heat paths is implemented with a piece of low thermal conductivity material (PEEK, 0.25 W/mK) fused in between two pieces of CC. The three block concepts have been simulated and measured as will be shown in the next sections.

2.1 Limitations of the thermal split

Whatever the quality of the heat path separation that is is achieved in the block, a residual coupling is still present through other routes.

There is a coupling between the detectors and the hybrid on the module by conduction through the location washer and glass fan-ins, which carries up to 0.23 W. But the dominant coupling is through the environment. Heat lost from the hybrid by convection and radiation tends to be picked up by the detectors because they have large area and low temperature.

The convective heat load on the detectors was investigated with a computational fluid dynamics (CFD) simulation [4] of a simplified geometry representing the space between two disks where gas can flow freely. The walls of this space were given a fixed temperature at the places where they are tiled with modules and assumed to be insulating elsewhere. The CFD simulation predicts a heat transfer to the detectors of outer modules which varies from 0.04 W at the bottom of the ring to 0.55 W at the top of the ring. Middle modules show a similar pattern to outers, with the range being from 0.16 to 0.55 W. Inner modules show the opposite pattern with the largest load being 0.22 W on the lowest modules and falling to 0.03 W at the top.

The most complete estimate of environmental heating comes from a thermal mock-up of a pair of facing disks [5]. A temperature difference of about 22 degrees was maintained between the

dummy hybrids and detectors, and the heat picked up by the detectors was measured. The mock-up showed that the heat picked up by outer modules is largest when the module is at the top of the wheel and is significantly larger for modules on high blocks than for those on low blocks. For these modules in the worst position, the average heating was 0.6 W with a measurement spread of 0.1 W. The pattern and magnitude of heat picked up by middle modules was very similar to that seen in outer modules. The power picked up by inner modules showed a rather large spread. There is some hint of the pattern seen in the CFD model where inner modules at the bottom of the wheel receive the most heat.

Based on these results we chose 0.2 W per detector as a safe upper limit [1] on the environmental heat load on any module type at any position on the disk. The only way to reduce this coupling is to reduce as much as possible the temperature difference between the hybrid and the detectors.

3 Module thermal simulations

The module is simulated with the FlexPDE package as described in [1]. This simulation includes all of the layers of material in the module, each with its nominal thickness and thermal conductivity, with the exception of the glue and grease layers for which worst cases are used. The glue between the detectors and the spine is simulated at the upper limit of its thickness (130μm) and the lower limit of its coverage (35%). The grease between the module and the cooling block is simulated at the upper limit of its thickness (30μm). Figure 4 shows the level of detail of the simulation.

The module simulation uses a simple parameterisation of the main cooling block performance, chosen to be slightly pesimistic compared with the measured performance of the 0.4mm PEEK split block at high power load:

$$T_h = 1.4P_h + 0.9P_d \qquad \text{and} \qquad T_d = 1.5P_d + 0.9P_h \tag{2}$$

where subscript $_{h(d)}$ represents the hybrid (detector) part of the block, P represents power and T represents temperature relative to the coolant. For outer modules the far end cooling block is simulated with a thermal resistance of 3.0 K/W between the block surface and the coolant. This is a conservative value based on simulations.
The estimated uncertainty on the simulated runaway point, considering the uncertainties on the material conductivities and on the boudary conditions, is about 15%.

Figure 5 shows the simulated runaway curve for inner and outer modules. Both simulations were run with the coolant temperature at -20 C, which is just low enough to put the runaway point above the specified value of 240 $\mu W/\mathrm{mm}^2$ at 0°C .

4 Evaporative cooling rig

The solution adopted to cool the SCT is based on a refrigerator cycle using C_3F_8 as evaporative fluid. The rig which supplied C_3F_8 for our measurements was designed and built at CERN

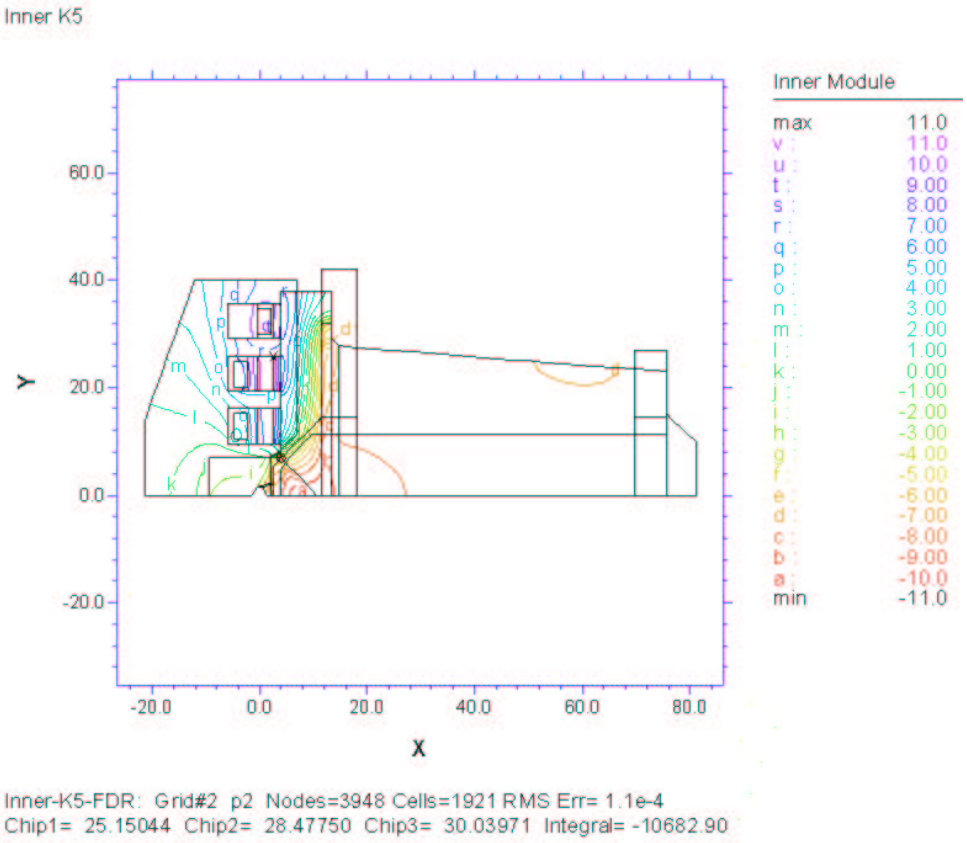

Fig. 4. Simulated temperature distribution of an inner module at maximum specified power.

with improvements added by RAL. For a complete description of the evaporative cooling rig see reference [6].

The C_3F_8 is compressed, cooled to room temperature, then further cooled before it is injected into a capillary. At the input of the capillary its pressure is around 5.5 bar and its temperature in the range of -15°C to -21°C . During its passage down the capillary its pressure drops to ∼1.5 bar, which is just below the saturated vapor pressu so shortly before reaching the end of the capillary it starts to boil. Then it enters a tube of 3.6 mm inner diameter and passes through a number of prototype cooling blocks followed by instrumented Cu blocks that are used to measure the Heat Transfer Coefficient (HTC). The capillary, the test structures and the Cu blocks are all in a freezer. The fluid then passes through a heater to evaporate any remaining liquid and then enters a collection tank. The collection tank provides gas at room temperature at the input of the compressor. The compressor speed is governed by a controller so as to maintain a constant pressure in the collection tank.

5 Heat Transfer Coefficient measurement

The heat transfer coefficient of C_3F_8 was measured over the range of conditions that we expect to use in the SCT cooling system [10]. Briefly these conditions are; mass flow rate between 1.6 and 2.2 g/s, cooling temperature between -20 and -26 C, vapour fraction between 10% and 80%, power density between 0 and 6 W/cm^2. The only one among these parameters which has a

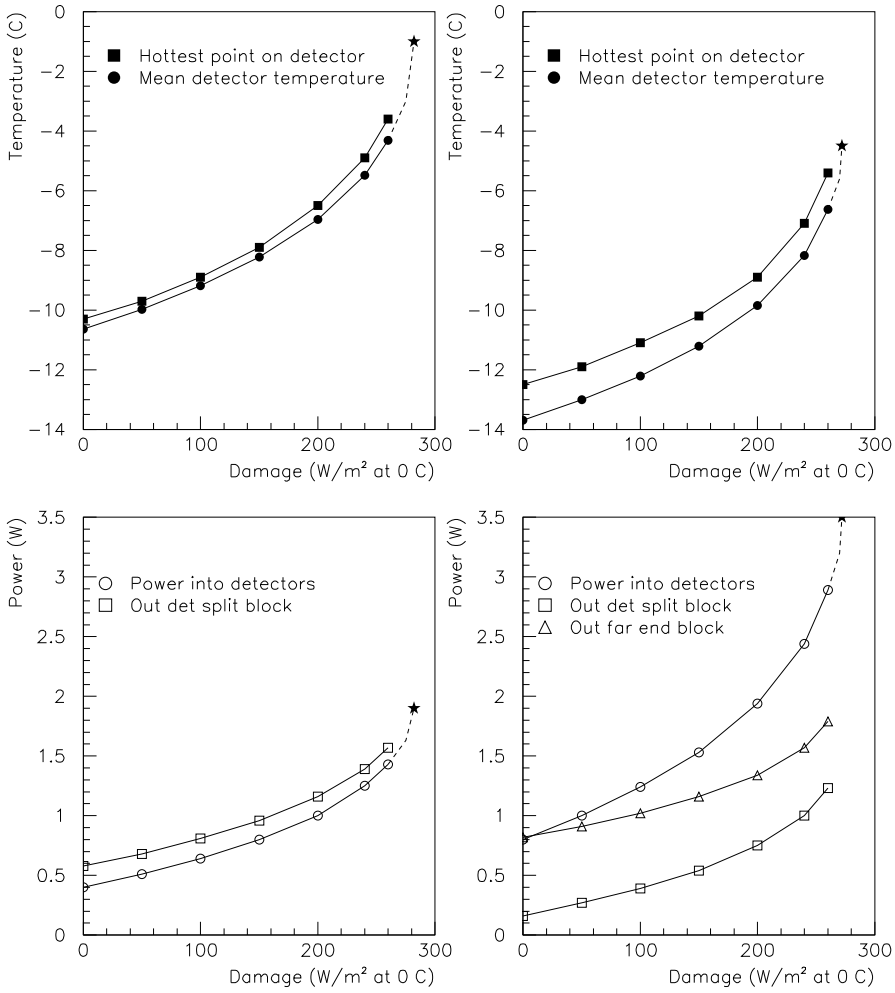

Fig. 5. Inner (left plots) and outer modules simulated with a coolant temperature of -20 C, a convective heat load of 0.2 W per detector and hybrid power of 6.8 W. The full FEA simulation is used for all points except the dashed line and star which shows the runaway point and is based on an extrapolation of the other points.

strong influence on the HTC is the power density. This rise of HTC with power density is an expected feature of boiling heat transfer. Figure 7 shows the HTC versus power density over a series of runs with varying conditions. There is some scatter from run to run which is larger than the estimated errors and is not explained. Nonetheless, all the data falls between the two straight lines represented by $H = 1800 + 330 \times D$ and $H = 2500 + 540 \times D$, so we use these upper and lower limits of the HTC as inputs to the cooling block simulations.

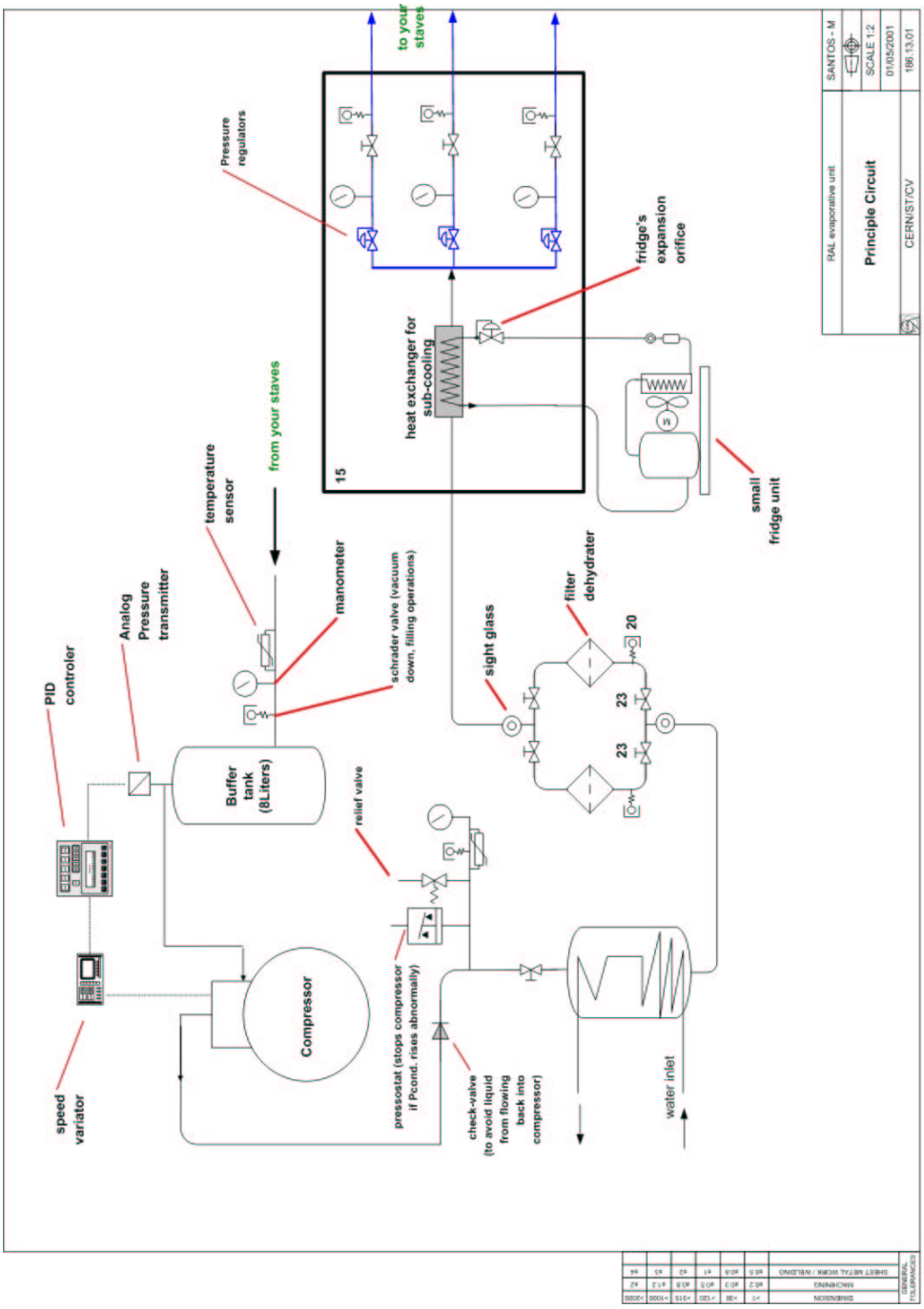

Fig. 6. Evaporative cooling rig schematics

6 Cooling block measurements and simulations

Three cooling structures have been tested with the evaporative cooling system. First was a series of five blocks of baseline design. The second was a series of three baseline and three fully split blocks. Finally, a single prototype PEEK split block was tested. In all tests the coolant flow conditions were within the range described in Section 5. Heaters were attached to the two surfaces of the block which contact the module and sensors were glued on to the block sides close to the heated surface. For details of the measurements and simulation see [11].

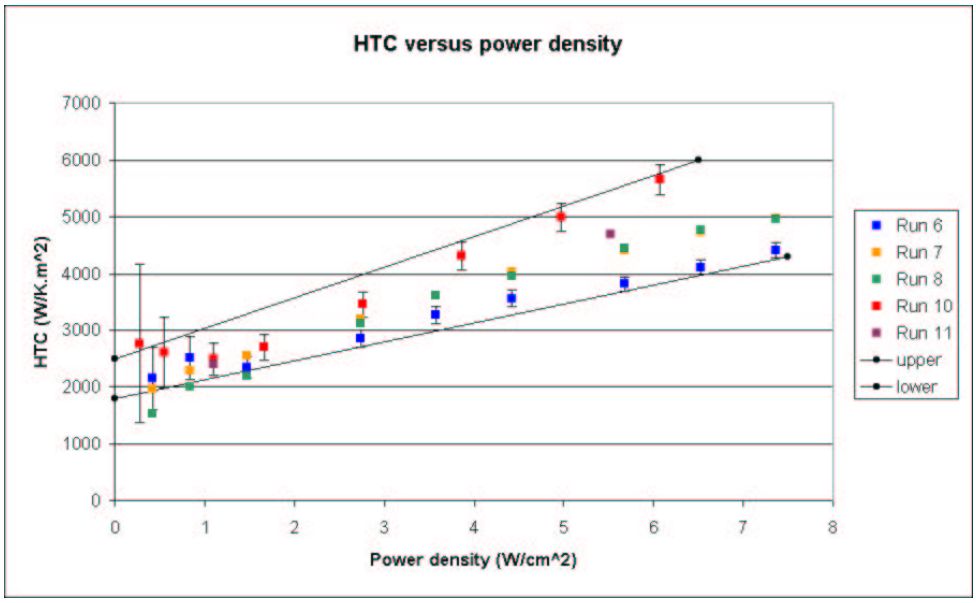

Fig. 7. Heat Transfer Coefficient measured versus power density.

The most important results are summarised in Figure 8. It shows the temperature of the detector half of the block when the maximum specified hybrid power (7 W) is applied to the hybrid half of the block. The detector block temperature is measured relative to the coolant and is plotted against the power applied to the detector half of the block. The maximum power that may have to be extracted by the detector block is 1.5 W for outer and middle modules and 2.0 W for inner modules. It can be seen that the 0.4mm PEEK split block shows an improvement of about 2 degrees over the baseline block and the fully split block offers a further improvement of almost 2 degrees.

In Figure 8 the measurements are compared with results from FEA simulations of various block designs. The simulation results have large error bars reflecting our uncertainty about the heat transfer coefficient. They cover the full range of HTC values described in Section 5. There is reasonable agreement between measurement and simulation for the baseline and 0.4mm PEEK designs. Also simulated is a split block with a 1mm PEEK layer which is expected to be almost as good as the full split and is more practical.

The agreement between measurement and simulation is not so good on the hybrid half of the block. On the baseline block the hybrid was measured to be almost three degrees cooler than expected from the simulation, while on the 0.4mm PEEK block the difference was five degrees.

7 Module measurements setup

The module used for these tests is the K5_313 inner module. This module has been irradiated at the PS 24 GeV proton beam up to the fluence of 1.5×10^{14} p/cm^2, annealed at 25°C for one week and then stored in a freezer at about -20°C . During the various measurements and shipping to different laboratories it is estimated that it remained at room temperature for an additional period of about 3 weeks.
The module has been kept electrically fully operational throughout the measurements. This

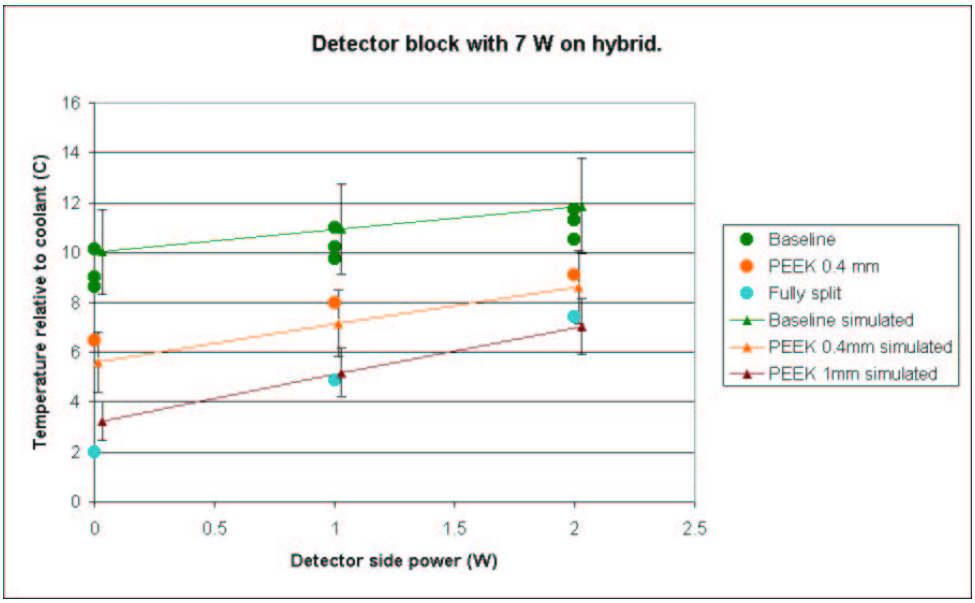

Fig. 8. Summary of the detector block performance.

means that high voltage was applied on the detectors and the readout electronics was powered and exercised via the SCT-DAQ. This module has a shunt shield implemented on the hybrid. The shunt shield is a thin foil of Cu connected to ground to improve the electrical isolation of the module and to improve its noise performance. Since the shunt shield frequently peels off, in the latest version of the hybrid, it has been removed. Preliminary electrical tests show that the performances are satisfactory. If further tests on the disk will indicate that the shunt shield is still needed, this will be implemented directly on the block thus improving its mechanical robustness.

The setup used for the thermal measurements aims at emulating the experimental environment where the module will have to operate. The relevant conditions to be controlled are the coolant temperature and the effect of convection and radiation on the detectors surface. The cooling blocks we used were soldered on a CuNi pipe and connected to the evaporative cooling rig at RAL, so as to replicate the real cooling interface between coolant and module. The convection and radiation conditions present in ATLAS are more difficult to emulate. The module is operating in a flushing nitrogen (N_2) atmosphere to avoid condensation on the detectors (relative humidity kept below 10% at any N_2 temperature), and placed in a dedicated test box inside a freezer. Both the temperature of the box and the temperature of the N_2 (through a heat exchanger) are set by the freezer temperature. Unfortunaly the freezer allows only a coarse regulation of its temperature and it was difficult to have stable conditions above zero degrees. It was not possible to use a climate chamber for the measurements at the evaporative cooling rig. The heat load from the environment on a module in ATLAS depends on the presence of all the other modules on the same disk. This load is not possible to emulate with our single module, so instead we aim at reducing the environmental heat load as close to zero as possible. This situation with a reduced convection can then be compared with a simulation in which the environmental load is set to zero. The best way to remove the convection would be to perform the measurements in vacuum. Two attempts have been made on the irradiated modules K5_307 (inner) and K5_305 (outer), but they both showed irreversible damage at the hybrid level when the detectors were biased at 500 V, probably due to discharge in the low pressure atmosphere (corona effect). So instead of using vacuum we maintained the freezer temperature close to the detectors temperature in order to minimise convection.

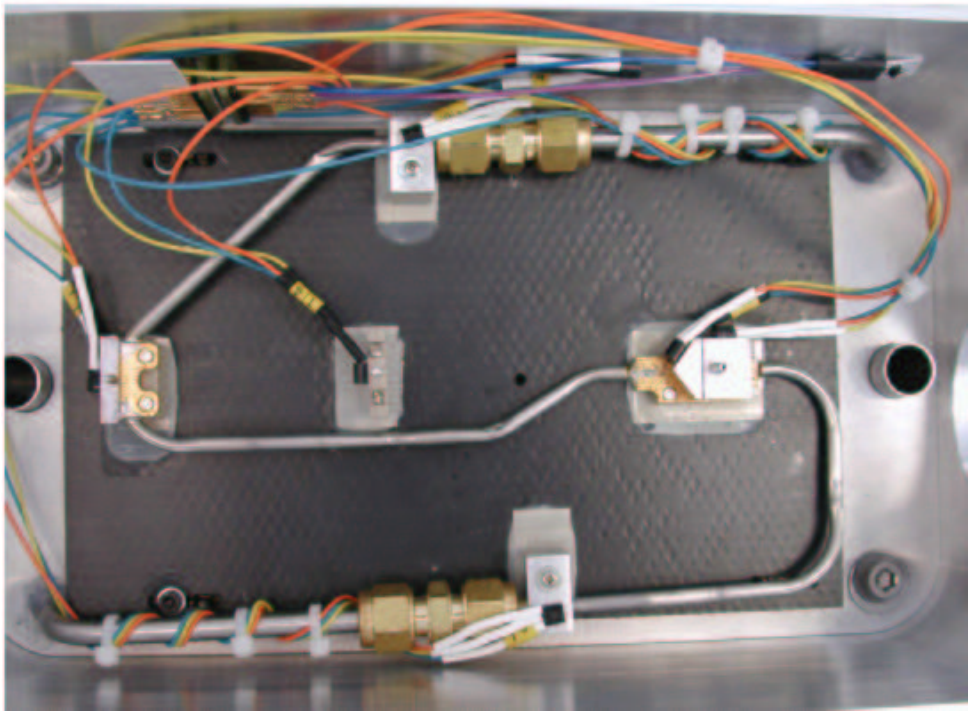

Fig. 9. Thermal box equipped with DS1820 sensors. Two cooling blocks are mounted on the cooling pipe and a PEEK support is fixed on the carbon fiber plate, allowing to measure both inner and outer modules. The relative humidity sensor (HIH3605 [7]) is also visible in the upper right corner.

The temperature regulation of the atmosphere inside the test box is crucial to obtain precise temperature measurements with the sensors we used. The module and environment temperatures are measured with DS1820 [8] glued at several critical points (see figures 9, 10) and readout with a dedicated LabView interface through a PointSix adapter. An ideal sensor would read the temperature of the surface onto which is glued, regardless of the environment conditions surrounding it. None of the existing sensors allow this feature because heat flows from the environment into the readout leads and from the leads into the sensing element itself. To overcome this inconvenience we developed a specific procedure consisting in a two steps calibration.
First, the DS sensors are thermally grounded to a large block of aluminum placed in a climate chamber. Setting the block at different temperatures allows to check the linear response of the sensors over a wide range of temperatures. Those sensors appear to have an excellent linearity in the interval of interest between -25°C and +25°C (see figure 11) Then a measurement of influence of the atmosphere temperature on the sensors read out is performed. The sensors are glued (with cyanolite) in their final position on the module (AlN wings) and in the box (see figures 9, 10). The chiller temperature is set to a fixed low value (about -20°C) and the atmosphere temperature is varied from -20°C up to a about +30°C . Since no power is injected in the module the temperature of the inlet, outlet and cooling block are in very good approximation at the same temperature of the coolant, while the detectors, due to their geometry (0.285 mm thick with a large area), change significantly their temperature during this operation. It is possible to observe from figure 12 that the measured value of the DS sensors varies significantly with increasing atmosphere temperature. The measured temperature, the real surface temperature and the atmosphere temperature are related in the following way:

$$T_{read} = T_{surface} + k(T_{atm} - T_{surface}) \tag{3}$$

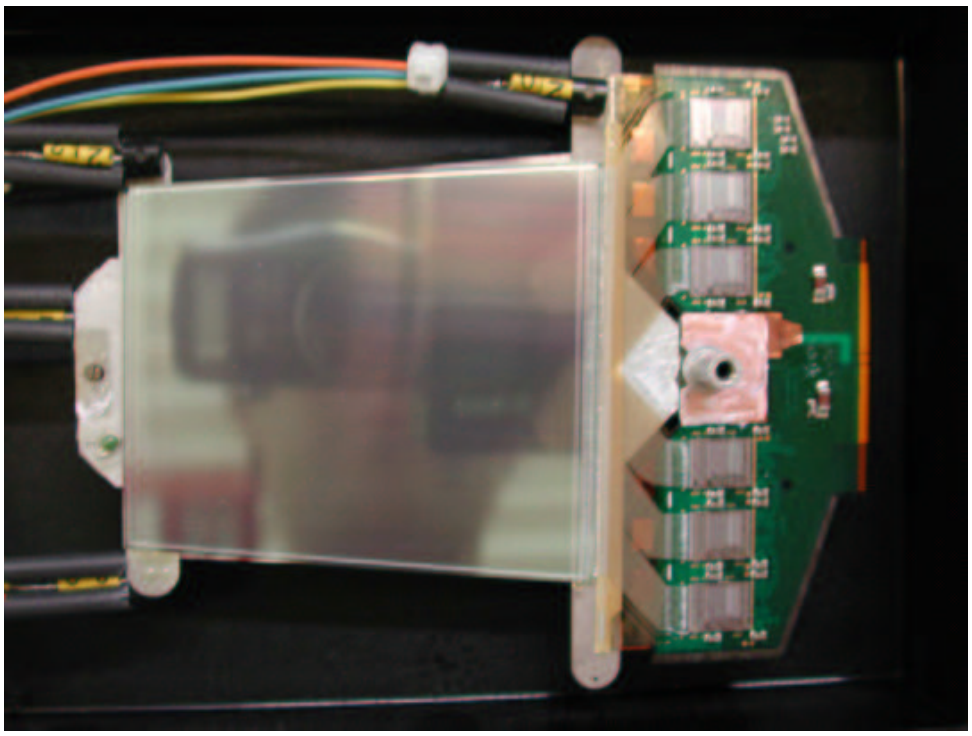

Fig. 10. DS1820 positions on the module. The module is upside-down showing the surface in contact with the cooling block. The shunt shield, partially covered with thermal grease is also visible.

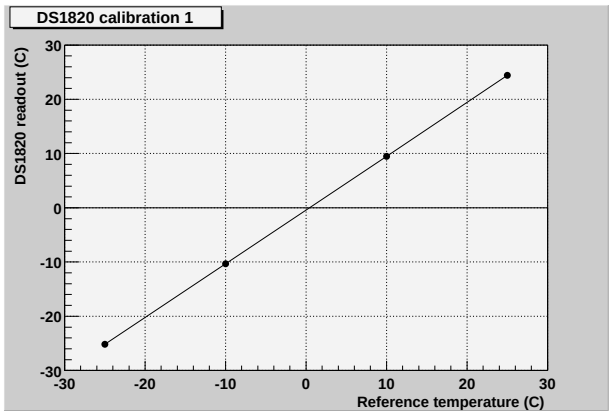

Fig. 11. Temperature values measured with a typical DS1820, plotted against the reference temperature.

where k is the slope fitted from the previous plot. From this equation it is possible to work out the real temperature of the surface:

$$T_{surface} = (T_{read} - T_{atm})/(1 - k) \tag{4}$$

The k values measured are reported in the following table.

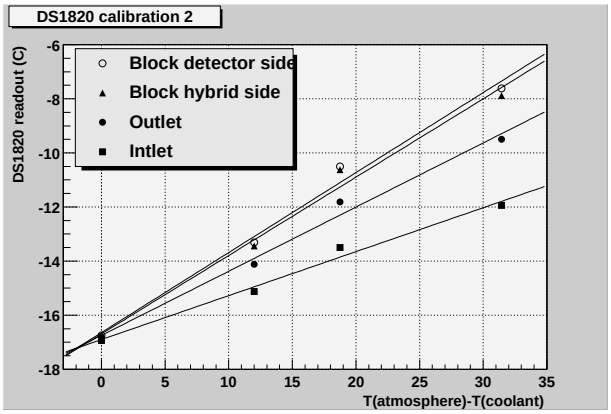

Fig. 12. Influence of the atmosphere temperature on the sensor readout value. In the plot the temperature read with the DS sensors is plotted against the temperature difference between the atmosphere and the real surface temperature assumed to be equal to the coolant temperature.

Position	k
inlet	0.16
outlet	0.23
block hybrid side	0.28
block detector side	0.28

Since, as explained before, the sensors glued onto the AlN wings of the detectors cannot be treated in the same way, the adopted procedure is to tune the temperature of the atmosphere to the temperature of the detectors to eliminate the heat flow from the environment to the sensors. During the temperature measurements at the evaporative cooling rig, where no climate chamber was available, we always tried to have at least the atmosphere slightly warmer than the detectors so as not to cool them with the N_2. For this reason the AlN wing temperatures measured have to be considered only as an upper limit to the real value, so that the analyzed situation can be cited as conservative.

8 Measurements results

Different runs at different conditions have been taken. The coolant temperature has been varied from -25°C to -14°C , while in all the measurements the temperature of the atmosphere has been set as close as possible to the detectors temperature to avoid any heat exchange. This situation should be as close as possible to the simulations, where no convection is considered. Two sets of measurements have been taken with the baseline block and the PEEK split block.
The following tables represent a summary of the data taken. The values of power injected into hybrid and detectors have been shown. Two temperatures are measured on the cooling block, on the hybrid and the detector sides. Four sensors have been glued on the AlN supports of the module (wings). The temperature of the detectors is well within 1°C of the temperature of the wings. This has been checked fixing temporary, with some thermal grease, a sensor directly on the strip surface of the detector. The power density is calculated knowing that the detector area

is 6180 mm^2 and it is normalized at 0°C using the wings temperature as mean value of the detector temperature in formula (1).
In the following tables the temperature of the wings is reported as readout from the sensors. In absence of a climate chamber, a fine tuning of the atmosphere temperature is practically impossible, so the atmosphere temperature has always been kept a little warmer than the detectors to avoid extracooling. For this reason, the reported wings temperatures have to be considered as an upper limit to the real values and appear with the symbol "<".

8.1 Run with the baseline block

	a	*b*	*c*	*d*	*e*
Hybrid power (W)	0.00	5.5	5.5	7.2	6.4
Detector Voltage (V)	0.0	0.0	495.8	494.9	490
Detector Current (μA)	0.0	0.0	375	451	856
Detector Power (W)	0.0	0.0	0.186	0.223	0.428
T Inlet/Outlet	-25.5	-24.4	-24.3	***-23.9***	-16.6
T hybrid	-	-2	-2	***3***	-
T block Hybrid side	-25.0	-11.9	-11.5	-8.7	-4.2
T block Detector side	-25.5	-13.7	-13.3	-10.8	-6.1
T wings	-	<-12.6	<-12.1	<***-10.7***	<-2.1
T box	-11.1	-10.4	-12.0	-10.0	1.9
T nitrogen	-9.9	-8.6	-9.4	-8.7	2.5
dPower (μW/mm^2 at 0°C)	0.0	0.0	< 105	< 108	< 85

In the first 4 runs the coolant temperature was set to -25°C . Run *a* has been taken with no power on the hybrid nor on the detectors, to have a reference point to be compared with the subsequent runs. In run *b* the hybrid has been powered to 5.5 W, which represents the typical power dissipation with chips biased at the voltages used during electrical tests (V_{cc}=3.5V, V_{dd}=4.0V). The detectors were unbiased. The ΔT between coolant and the hybrid side of the block is around 12°C , and the difference between the two halves of the block is around 2°C . In run *c* the detectors power is about 0.19 W. The temperatures of detectors and block are almost unchanged with respect to run *b*.
In run *d* the power on the hybrid has been increased to the maximum of 7.2W, to test whether the module meets the specifications. This value has been obtained increasing the chip voltages to their limits (V_{cc}=4.2V, V_{dd}=4.2V), and repeating trigger bursts at 1fC threshold [9]. The two sides of the block keep a temperature difference of 2°C and the detectors are running cooler than -10°C . The hybrid is close to the target value of +2 degrees.
In run *e* the powers were 6.4 W on the hybrid and 0.4 W on the detectors. The environment has been considerably warmed up. The coolant temperature set to about -16°C , close to the highest temperature reachable with the evaporative cooling rig, and the atmosphere around +2°C . This

test was performed to check the module thermal stability. The detectors were running stably below 2°C and the difference between the two halves of the block remained at 2°C .
In all the performed tests the power density at 0°C on the detectors is about $100\mu W/\mathrm{mm}^2$ at 0°C while the one cited in the specifications is $185\mu W/\mathrm{mm}^2$ at 0°C . In the results discussion, a scaling procedure will be applied to check whether the module is within the specifications.

8.2 Run with the PEEK split block

	a	*b*	*c*	*d*	*e*	*f*	*g*
Hybrid power (W)	0.0	6.5	6.5	0.0	6.4	6.4	6.4
Detector Voltage (V)	0.0	0.0	494.6	0.0	0.0	492.0	489
Detector Current (μA)	0.0	0.0	485	0.0	0.0	0.713	940
Detector Power (W)	0.0	0.0	0.24	0.0	0.0	0.37	0.470
T Inlet/Outlet	-24.6	-24.3	***-23.4***	-14.5	-14.4	-13.6	-14.3
T hybrid	-	6	***6***	-13	9	10	10
Tblock Hybrid side	-24.6	-7.7	-6.4	-14.5	-1.5	-0.3	-2.5
Tblock Detector side	-24.5	-12.6	-10.7	-14.5	-6.5	-4.8	-6.7
T wings	-	<-11.5	***<-10.3***	<-11.6	-	-	<-1.7
T box	-11.5	-10.4	-10.2	-8.8	-8.1	-8.0	1.4
T nitrogen	-8.8	-6.6	-8.9	-8.5	-6.5	-9.2	2.5
dPower ($\mu W/\mathrm{mm}^2$ at 0°C)	0.0	0.0	< 113	0.0	0.0	< 107	< 90

The same module has been mounted on a PEEK split block, in the same setup. In the first three runs the coolant temperature has been set to -24°C . The first run was performed with no power on the module, to have a reference point to be compared with the subsequent runs. In run *b* the hybrid have been powered to 6.5W. The hybrid side of the cooling block increases its temperature to about -8 degrees. The temperature difference between the two halves of the block is about 5°C . The detectors are around -11°C , unbiased. When in run *c* the detector power is 0.24 W their temperature is almost unchanged, and the temperature difference across the block is about 4.3°C . In both cases the hybrid temperature is around 6°C .
In runs *d,e,f* the coolant temperature has been increased up to -14°C , to check the module thermal stability. The module didn't show any sign of thermal runaway when fully biased and the temperature difference between the two halves of the block was still around 5°C .
In run *g* the atmosphere temperature has been increased up to 2.5 degrees. The detectors were running stably below -2°C dissipating 0.47W and the temperature difference across the block was around 4.2°C .
As in the previous section, in all the performed tests the power density at 0°C on the detectors is about $100\mu W/\mathrm{mm}^2$ at 0°C while the one cited in the specifications is $185\mu W/\mathrm{mm}^2$ at 0°C . In the results discussion, a scaling procedure will be applied to check whether the module is within the specifications.

9 Discussion of results

The inner module has been mounted on two different cooling blocks to validate its thermal design and to understand which is the best cooling block to be used in the experiment.
A direct comparison of the performance of the module mounted on the two different blocks is possible looking at the run *d* of the baseline block versus the run *c* of the PEEK split block. The environment temperature is almost equal. Even though the power dissipated by the hybrid is 6.5 W during the tests on the PEEK split block but 7.2W during the runs on the baseline block the hybrid temperature when the module is mounted on the PEEK split block is 3°C warmer.

	baseline block	peek split block
Hybrid power (W)	7.2	6.5
Detectors power (W)	0.22	0.24
ΔT(hybrid-coolant)	26°C	29°C
ΔT(detectors-coolant)	<13°C	<13°C
ΔT(Hybrid-detectors)	>14°C	>16°C
ΔT(across the block)	2°C	5°C

Since, as explained above, with this setup it is only possible to set an upper limit on the detectors temperature, the temperature difference between the coolant and the detectors, when the module is fully biased, is < 13°C irrespective of the block we used. This effect could still be attributed to a coupling between hybrid and detectors through the fanins and to a remaining coupling through the block. Since it would be unrealistic to change the design of the module at this stage of the project it has been decided to increase the actual PEEK thickness from 0.4mm to 1mm, improving the separation between the detectors and hybrid heat paths.
The detector radiation damage of this module is about 100 $\mu W/\mathrm{mm}^2$ at 0°C . In the runaway specifications the considered value, including a safety margin, is $240\mu W/\mathrm{mm}^2$ at 0°C . As explained in Appendix A, the temperature reduction that is necessary in order to compensate the power density difference from $100\mu W/\mathrm{mm}^2$ at 0°C to 240 $\mu W/\mathrm{mm}^2$ at 0°C is 8.4°C . Therefore if we reduce the coolant temperature by this amount and simultaneously increase the radiation damage to the SCT maximum then the detector temperature relative to the coolant would be unchanged. Rescaling the PEEK split block run *g* in this way, the coolant would be at about -23°C and the detectors at about -10°C . To this estimate it is necessary to add the contribution coming from the convection, deliberately made negligible in our measurements. It has been predicted that the heat load on an inner module will be around 0.4 W [4]. According to the measured inner module thermal resistance of 4.5 K/W between detector and block [1], this would increase the detectors temperature by about 2°C to -8°C , a value that still meets the specification. Some further improvements could be applied on the hybrid side of the cooling block to reduce the hybrid temperature that is above the target value of 2°C . It would be possible, for instance, to increase the pipe coverage with a longer straight section on the hybrid half.

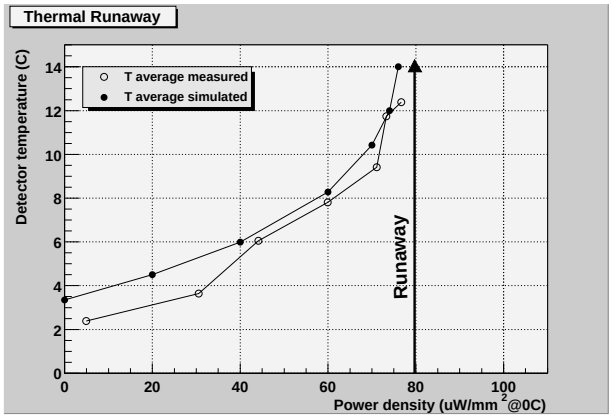

Fig. 13. Measured thermal runaway plot.

10 Thermal runaway

A dedicated test to measure the thermal runaway point has been performed. Since it was impossible to observe any sign of thermal runaway with the evaporative cooling rig, it has been decided to use a conventional liquid based chiller to obtain a warm enough coolant temperature.

10.1 Measurements setup

The set up differs from the one used at the evaporative cooling rig in only a few respects.
The module was still mounted on the peek split cooling block in the same dedicated box but, to better control the atmosphere temperature, it has been possible to install the box in a climate chamber. The nitrogen flowing in the box was cooled via a heat exchanger mounted in the climate chamber. With this solution it is possible to keep the module in a dry atmosphere, avoiding condensation and, most important, to tune the box and the atmosphere temperature to the surface temperature of the detectors. This reduces any heat exchange of the detectors with the environment, and most important allows to control the atmosphere influence on the DS1820 readout, a condition very difficult to reach in the freezer used for the evaporative runs. The coolant we used is a commercial antifreeze. The temperature of the coolant at which the runaway occurs is difficult to predict from simulations since the heat transfer coefficient of this liquid to the CuNi pipe has not been measured. The attempt at -5°C allowed us to observe the phenomenon.
The runaway point was reached by looping on a sequence of steps. The chiller was set to -5°C . When it reached the equilibrium the front end electronics was turned on to 6.5 W and the climate chamber has was set at the equilibrium temperature of the unbiased detectors. Then the path to the runaway point starts by increasing the bias on the detectors. After any variation of the detector bias the thermal equilibrium has to be reached. This is a lengthy procedure. The climate chamber has to be set to the detector temperature, but changing the temperature of the atmosphere results in a modification of the detector temperature; this loop may be repeated a few times until it converges to a final equilibrium. In figure 13, the measured average wings temperature and the simulated average detector temperature has been plotted as a function of the power density normalized to 0°C . The simulation takes the measured block temperatures in the runaway experiment as input. It has zero convection heat load, 6.5 W hybrid power. All other details are exactly as described in section 3. The thermal runaway point is represented in

V det supply (V)	V det (V)	Ileak μA	Power (W)	dP $\mu W/\mathrm{mm}^2$ at 0°C	T wings (max) (°C)	Simulated Twings (°C)	Tatmosphere (°C) (°C)
50	39	1002	0.04	5	2.5	3.35	2.81
200	182	1566	0.29	31	4.19	4.5	3.12
275	252	2047	0.52	44	6.44	5.99	5.75
350	321	2559	0.82	60	8.06	8.28	7.19
400	364	3187	1.16	71	9.81	10.42	8.44
420	374	4130	1.54	73	12.38	11.99	10.19
425	374	4630	1.73	77	13.06	14	11.06

Table 1
V det supply is the voltage delivered by the HV power supply; V det is the voltage applied to the detectors once the voltage drop on the HV filter (equivalent to a 11.2 kΩ resistor in series) is subtracted; Power is the power dissipated on the detectors once the power drop on the HV filter is subtracted; dP is the power density on the detectors normalized to 0°C ; Twings is the maximal temperature measured on the AlN wings; Simulated Twings is the maximal temperature on the detectors obtained from the simulations; Tatmosphere is the temperature of the N_2 flushing in the box.

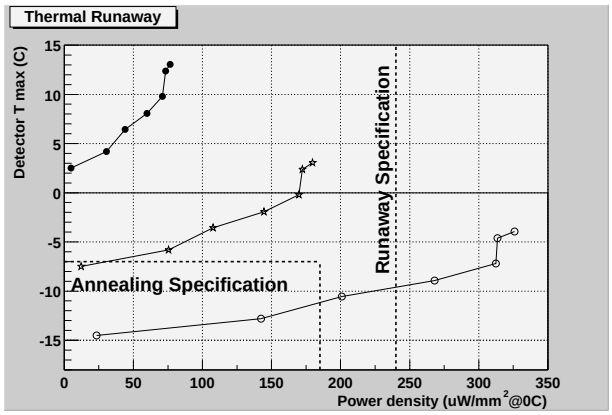

Fig. 14. Rescaled thermal runaway plot to different coolant temperatures: black dots (measured) Tcool=-5°C , stars Tcool =-15°C , open dots Tcool=-22°C

this kind of plot as a vertical asymptote, where the module cannot reach thermal equilibrium. It is visible from the plot that the runaway curve reaches the expected asymptote at a power density around 80 $\mu W/\mathrm{mm}^2$ at 0°C .
This value can not be compared directly with the values set in the specifications since the operating temperature is much warmer than that expected in the experiment, the heat transfer coefficient of the monophase liquid is different from the evaporative system and the power density at 0°C on the detectors is around 80 $\mu W/\mathrm{mm}^2$ at 0°C instead of $240\mu W/\mathrm{mm}^2$ at 0°C required by the thermal specifications. It is possible to rescale analytically the measurement we performed at -5°C to the expected -22°C and increase simultaneously the power density at 0°C on the detectors, see figure 14. The analytical rescaling is explained in Appendix A. Figure

14, shows the rescaled runaway plot with the specifications values. The detectors should run cooler than -7°C up to $185\mu W/\mathrm{mm}^2$ at 0°C (annealing specification). The plot shows that the detectors are at about -10°C when the coolant temperature is -22°C . This value doesn't take into account the heat load coming from convection; as already shown in the previous section this will increase the detectors temperature of about 2°C leaving the module within the specifications. The runaway point is well above the specification value of $240\mu W/\mathrm{mm}^2$ at 0°C even with the lower heat transfer coefficient of the monophase liquid coolant. This positive result has anyway to be considered as a measurement performed on a sample of one module.

11 Conclusions

The inner module represents the most critical thermal design on the SCT disk because it has only one detector cooling point.
To validate this design one inner irradiated module has been analyzed. The module has been tested at different coolant temperatures with the evaporative cooling prototype at RAL and mounted on different cooling blocks. The radiation damage measured knowing the power dissipated by the detectors and their temperature is around $100\mu W/\mathrm{mm}^2$ at 0°C . The temperature measurements properly rescaled to the radiation damage of $240\mu W/\mathrm{mm}^2$ at 0°C set in the specifications lead to a required coolant temperature of the SCT endcaps at full irradiation around -23°C , when mounted on the peek split block. Considering a convection heat load of 0.4W on the detectors, the expected detectors temperature is -8°C . The hybrid temperature is around +6°C , a few improvements could still be applied on the hybrid half of the cooling block to reduce this value.
The runaway point measured with a monophase liquid coolant at -5°C is around $80\mu W/\mathrm{mm}^2$ at 0°C ; rescaling the measured value to a coolant temperature of -22°C would lead to a runaway point above $300\mu W/\mathrm{mm}^2$ at 0°C . It remains necessary to measure a larger sample of blocks and modules to assure the reproducibility of this performance.

12 Acknowledgements

We would like to thank the following people for their contributions to this work: Lewis Batchelor, Stephen Haywood, Christian Hirt, Tim Jones, Hans-Guenther Moser, Ray Thompson and Maarten Weber.

A Radiation damage rescaling

Few prototype modules have been irradiated at different fluences. To observe the runaway of modules exposed to low fluence, it is often useful to run them at a warm coolant temperature. Once the runaway point is found, it is then necessary to rescale the measured power density, to a (usually) cooler coolant temperature.
It is possible to express this problem in the following way. Let's assume a practical case: coolant set to -5°C , detectors temperature +12°C and detectors power dissipation of 2W. Now we want to know the corresponding temperature of the detectors with a different coolant temperature for example -20°C ($\Delta T_{coolant}$=15°C), in the same power conditions. The ΔT between detectors and coolant is 17°C with a power dissipation of 2W.
The leakage current is a function of the temperature; it can be approximated as

$$I(T) = I(T_0)2^{(\frac{T-T_0}{7})} \tag{A.1}$$

where T_0 is any reference temperature. The power dissipated by the detectors follows the same relation. To keep the same ΔT the detectors have to dissipate 2W at the new coolant temperature of -20°C . Since the leakage current decreases with the temperature, I can artificially increase the power dissipation at 0°C to balance it.
In order to do this I can scale the radiation damage in the following way:
the value I measure is

$$P(12°C) = P(0°C)2^{\frac{12}{7}} = 2W \tag{A.2}$$

the power dissipation at -3°C is

$$P(-3°C) = P(0°C)2^{\frac{-3}{7}} \ll 2W \tag{A.3}$$

I require $P(-3°C) \rightarrow$2W.
I can write

$$2W = P(0°C)(2^{\frac{12-(-3)}{7}})2^{\frac{-3}{7}}. \tag{A.4}$$

Now I define

$$P'(0°C) = P(0°C)2^{\frac{12-(-3)}{7}} \tag{A.5}$$

or in general

$$P'(0°C) = P(0°C)2^{\frac{\Delta T_{coolant}}{7}} \tag{A.6}$$

including as radiation damage the factor coming from the temperature dependence. $P'(0°C)$ is the radiation damage I would need, to have $\Delta T = 17$°C between detectors and coolant, at a

different coolant temperature.
Now

$$P'(-3°C) = P'(0°C)2^{\frac{-3}{7}} = 2W \tag{A.7}$$

In this way it is possible to map each point of the runaway plot (detectors temperature, power density at 0°C) taken at any coolant temperature to the correspondent one at a different coolant temperature.

$$\begin{pmatrix} T \\ P(0°C) \end{pmatrix} \rightarrow \begin{pmatrix} T - \Delta T_{coolant} \\ P(0°C)2^{\frac{\Delta T_{coolant}}{7}} \end{pmatrix}$$

References

[1] Snow, S., Thermal and Mechanical Specifications and Expected Performance of the Forward SCT Module. *ATL-IS-EN-0007* (2002)

[2] Anghinolfi, F., private communication

[3] Moore, A.V., Highly Oriented Pyrolitic Graphite and its Intercalation Compounds. Chemistry and Physics of Carbon, v.17, pp233-304 (1981)

[4] Fowler, R.F. CFD Simulations of convection in the Atlas Forward Silicon Tracker.

`http://hepwww.rl.ac.uk/Atlas-SCT/engineering/ec_fdr/misc/convection_v2.pdf`

[5] Thompson, R, et al Measurements of convection between the disks of the ATLAS SCT end cap.

`http://www.hep.man.ac.uk/groups/atlas/TM/CONVECTION8.DOC`

[6] ST/CV Group Cooling of electronics & Detectors

`http://st-support-cooling-electronics.web.cern.ch/st-support-cooling-electronics/`

`CoolingSystemWeb/RALUnit/RALEvapUnit.htm`

[7] HIH3605 Humidity sensor

`http://content.honeywell.com/sensing/prodinfo/humiditymoisture/009012_2.pdf`

[8] DS1820 Temperature sensor

`http://www.maxim-ic.com/quick_view2.cfm/qv_pk/3021/ln/en`

`http:/pdfserv.maxim-ic.com/arpdf/DS1820-DS1820S.pdf`

[9] ABCD3T Documentation

`http://chipinfo.web.cern.ch/chipinfo/`

`http://chipinfo.web.cern.ch/chipinfo/docsabcd3t_spec_v1.2.ps`

[10] Snow, S. et al The C_3F_8 evaporative heat transfer coefficient.

`http://www.hep.man.ac.uk/groups/atlas/TM/RALhtc.doc`

[11] Wilmut, I. et al Tests of forward SCT cooling blocks with C_3F_8 evaporative cooling.

`http://www.hep.man.ac.uk/groups/atlas/TM/RALblock.doc`